

**Competitive removal of hazardous dyes from aqueous solution by MIL-68(Al); Derivative spectrophotometric method and response surface methodology approach**

Mahnaz Saghanejhad Tehrani, Rouholah Zare-Dorabei <sup>\*\*</sup>

*Research Laboratory of Spectrometry & Micro and Nano Extraction, Department of Chemistry, Iran University of Science and Technology, Tehran 16846-13114, Iran*

---

\* Corresponding author.:  
Tel.: +98-21-77240516  
Fax: +98-21-77491204  
E-mail address: Zaredorabei@iust.ac.ir

## Abstract

MIL-68(Al) as a metal organic framework (MOF) was synthesized and characterized by different techniques such as SEM, BET, FTIR, and XRD analysis. This material was then applied for simulations removal of Malachite Green (MG) and Methylene Blue (MB) dyes from aqueous solutions using second order derivative spectrophotometric method (SODS) which was applied to resolve the overlap between the spectra of these dyes. The dependency of dyes removal efficiency in binary solutions was examined and optimized toward various parameters including initial dye concentration, pH of the solution, adsorbent dosage and ultrasonic contact time using Central Composite Design (CCD) under Response surface methodology (RSM) approach. The optimized experimental conditions were set as pH 7.78, contact time 5 min, initial MB concentration 22 mg L<sup>-1</sup>, initial MG concentration 12 mg L<sup>-1</sup> and adsorbent dosage 0.0055 g. The equilibrium data was fitted to isotherm models such as Langmuir, Freundlich and Tempkin and the results revealed the suitability of the Langmuir model. The maximum adsorption capacity of 666.67 and 153.85 mg g<sup>-1</sup> was obtained for MB and MG removal respectively. Kinetics data fitting to pseudo-first order, pseudo-second order and Elovich models confirmed the applicability of pseudo-second order kinetic model for description of the mechanism and adsorption rate. Dye-loaded MIL-68(Al) can be easily regenerated using methanol and applied for three frequent sorption/desorption cycles with high performance. The impact of ionic strength on removal percentage of both dyes in binary mixture was studied by using NaCl and KCl soluble salts at different concentrations. According to our findings, only small dosage of the proposed MOF is considerably capable to remove large amounts of dyes at room temperature and in very short time that is a big advantage of MIL-68 (Al) as a promising adsorbent for adsorptive removal processes.

**Keywords:** Metal-Organic Framework; Methylene Blue; Malachite Green; Competitive Adsorption; Derivative spectrophotometry; Response surface methodology

## 1. Introduction

Dyes and pigments which are regarded as a category of hazardous materials, are consuming by production and relevant industries such as textile, leather, plastic, food processing, cosmetics, paper, printing, pharmaceutical and dye manufacturing industry [1,2]. During the past years, these organic pollutants have attracted a lot of attentions due to their serious toxic effects on environment, human health and animals even at low concentrations [3,4]. Malachite green (MG) is a kind of triphenylmethane dye, which has been widely used in disinfection processes and in aquaculture industry to treat scratch on the fish bodies and to defend against bacterial infections [5-7]. However, since 1990s, MG's applications have been strictly limited because of its highly toxic, persistent, carcinogenic, and mutagenic properties [7]. Although its significant adverse effects, Methylene blue (MB), a well-known cationic dye, is used in various industries as coloring agent and redox indicator in analytical chemistry and medical applications [8,9]. Common properties of MG and MB dyes are listed in Supplementary content (Table S1).

All mentioned problems make it necessary to introduce effective treatment methods to control the dyes concentration in water sources especially water-soluble ones which tend to pass through the conventional treatment systems. Among the numerous physical, chemical and biological treatment techniques, adsorption has been extensively utilized to remove dye compounds in aqueous environments. This method is benefitted from unique advantages such as high efficiency, simplicity and large scalability [10,11]. Various adsorbents, such as activated carbon [12-14], polymeric materials [15-17], agro-industrial wastes like sawdust, rice husk and also biosorbents (such as biomass and chitosan) which are regarded as low cost adsorbents [18-20], nanocomposites [2, 21-23], graphite oxide [24,25] and porous adsorbents such as activated carbon [12-14], carbon molecular sieves [26], zeolites [27] and metal organic frameworks [28,29] have been reported for dye uptake in the literature. Among these proposed adsorbents, porous materials represent large

surface area, high reactivity and strong adsorption affinity to aqueous adsorptive removal of pollutants [30-33].

Metal-organic frameworks (MOFs) are porous and crystalline three-dimensional networks comprising mono- or multinuclear transition metal centers connected coordinatively through multifunctional organic linkers. Due to their remarkable surface areas, modifiable pore size, pore distribution and pore architecture, MOFs are promising alternative for gas storage, drug delivery, sensing and challenging adsorptive separations [34-36]. According to our knowledge, in spite of valuable applications of MOFs, there are a few reports on the adsorptive behavior of these materials for dye removal [29, 37-39]. MIL-n materials are a class of MOFs comprised from trivalent metal cations such as  $\text{Al}^{3+}$ ,  $\text{Cr}^{3+}$ ,  $\text{V}^{3+}$ ,  $\text{In}^{3+}$  or  $\text{Ga}^{3+}$  and carboxylic acid groups [40]. The three-dimensional networks of MIL-68 (Al) feature two kinds of channels with an opening diameter of 6.0– 6.4  $\text{\AA}$  and 16–17  $\text{\AA}$  exhibiting high surface area and sufficient thermal stability [41].

It is important to imply that, many industrial effluents are composed of several dyes; however, a little information is recorded about the simultaneous removal of multi-component dye compared with various researches applied for removal of single component textile dyes in the literature. Overlapping between the spectra of dyes is an important problem while studying of the dyes mixture simultaneously [42]. Among many analytical techniques, derivative spectrophotometry is defined as a robust and suitable option to resolve the problem of overlapping. The background of signals originated from the presence of other components in sample can be omitted by this method [43].

In customary methods, one factor at a time approach is generally time consuming and non-feasible to give the true optimum conditions because of requiring high number of experiments and the lack of interactions among the factors [44]. In recent years, statistical experimental design enables the researchers to achieve useful information on the effect of variables individually and/or the possible interaction between them based on mathematical modeling leading to decrease the process development time, overall costs and the number of experiments [45,46]. Nowadays, central

composite design (CCD) under response surface methodology (RSM) is a statistical tool to estimate main effects and interaction of the variables. A useful predictive model is then obtained for first or second order polynomial equations to the experimental responses in the experimental design followed by analysis of variance (ANOVA). In this way, the real optimal conditions can be found with respect to the tridimensional graphs. Significance of process variable will be analyzed by p-value and F-value parameters [46].

This research is of great importance because of working on: (a) the application of the micro/mesoporous metal organic frameworks as adsorbent in separation systems, (b) binary solutions of dyes, which is a notable challenging subject especially in real sample analysis, (c) experimental design methodology to give more accurate knowledge about the interaction between variables and to achieve the optimal conditions with less time elapsed while requiring lower number of experiments in compared with the one-factor at the time conventional method. After finding the optimal conditions by chemometric tools, kinetics and isotherm studies corresponding to dyes adsorption were performed in order to obtain some useful variables such as maximum adsorption capacity of the adsorbent and rate constants.

Finally, the reusability of the dye-loaded sorbent followed by the effect of ionic strength on removal efficiency of the proposed MOF was discussed in detail.

## **2. Experimental**

### **2.1. Materials and instrumentation**

All reagents including Terephthalic acid,  $\text{AlCl}_3 \cdot 6\text{H}_2\text{O}$ , HCl, NaCl, NaOH, methanol, Methylene Blue and Malachite Green were of the best available analytical reagent grade and supplied from Merck Co. An accurately weighted amount of MG or MB was dissolved in deionized water (1000 mg  $\text{L}^{-1}$ ) as stock solution and the working concentrations was prepared by suitable diluting this solution. The pH of sample solution was adjusted by addition of dilute HCl or NaCl solution. The

mixture solution for simultaneous competitive dye uptake was prepared by addition of appropriate increment of their stock solution.

A Metrohm pH meter with a combined double junction glass electrode was used for pH measurements. The absorbance spectra for MG and MB dyes was recorded in the range of 450 nm to 750 nm using T80+ UV-Vis spectrophotometer. Second order derivatives of the spectra of the mixtures were used in order to study the binary solutions. The linear calibration curve at maximum wavelength of each dye (defined by derivative spectrophotometric method) was obtained by plotting absorbance toward MB or MG concentration over desired concentration range. An ultrasonic bath with heating system (Elmasonic model) was utilized for the ultrasound-assisted removal procedure. X-ray diffraction (XRD) pattern was recorded by an automated Philips X'Pert X-ray diffractometer with Cu Ka radiation (40 kV and 30 mA) for  $2\theta$  values over  $5-40^\circ$ . Fourier transform infrared spectroscopy (FT-IR in the range of  $400-4000\text{ cm}^{-1}$ ) of the adsorbent was recorded using FT-IR spectrophotometer (Model: Shimadzu-8400S, Japan) at room temperature. The morphology of the adsorbent was observed by SEM (scanning electron microscopy; Tescan Vega II) method under an acceleration voltage of 15 Kv. The BET (Brunauer, Emmett, and Teller) surface areas of the adsorbent was measured using ASAP 2020 (Micromeritics Instrument Corporation) surface area analyzer where  $\text{N}_2$  gas was used as adsorbate. Prior to measurement, the adsorbent was degassed at 423 K for 12 h. The surface area of MIL-68(Al) was calculated by BET method. In order to investigate the thermal stability of the sorbent, thermogravimetric analysis (TGA) was performed using STA 504 instrument. Sample was heated at rate of  $5\text{ Kmin}^{-1}$  to 873 K under air flow and its approximate weight was 10 mg. Design-Expert, a statistical software package 7.0 was used for experimental design analysis and their subsequent regression analysis. The quality of the polynomial model equation was judged statistically by the coefficient of determination  $R^2$  and its statistical significance was determined by F-test. P-values less than 0.05 were considered to be significant.

## 2.2. Preparation of MIL-68(Al)

The synthesis and the activation process were performed by following the conditions reported previously in our submitted article as well as in the literature [41]. Briefly terephthalic acid (1.67 g; 10 mmol) and  $\text{AlCl}_3 \cdot 6\text{H}_2\text{O}$  (1.63 g; 6.74 mmol) were dissolved separately in 50 mL of DMF (94.4 g; 1292 mmol). The mixture was placed in a round bottom flask equipped with a condenser and was kept stirring and heated for 18 hours at 398 K under air. The mixture was then slowly returned to room temperature. The yellow solid was recovered by filtration. In order to remove the free acid which can remain in the pores, the as synthesized product was dispersed in  $3 \times 25$  mL of DMF under ultrasonic radiation (at  $35^\circ\text{C}$ ). To further remove the DMF out of the pores, the same procedure was repeated four times using  $4 \times 25$  mL of MeOH instead of DMF. The as-synthesized MIL-68(Al), after filtration, was dried overnight in  $200^\circ\text{C}$  under vacuum and stored in a desiccator.

## 2.3. Multi-component adsorption of MG and MB dyes on MIL-68(Al)

All experiments were carried out in binary system of MG and MB using specified amounts of each dye solution (25 mL) of desired concentration and pH 4.5-10.5 with a known amount of adsorbent (0.001-0.007 g) loaded into 50 mL flasks. Thereafter, the flask was maintained in an ultrasonic bath for specific time intervals (2-10 min) at room temperature. The mixtures were then centrifuged at 6000 rpm for 5 min to minimize interference of the MOF fines with the analysis. Finally, the sample was taken for UV–Vis analysis. Second order derivative of the absorbance spectra was used to obtain the optimal wavelength at which the impact of the other component was minimized. The optimal wavelengths for measurement the concentration of each dye in binary solution were found to be 594 nm and 692 nm for MG and MB respectively. The efficiency of dye removal was determined in different experimental conditions according to CCD method. The isotherm and kinetics of the adsorption were determined by measuring the adsorptive uptake of the dye in various

initial dye concentrations and at different time intervals under optimum conditions respectively.

The dye removal percentage (R%) was calculated using the following relationship [47]:

$$Removal\% = \frac{C_0 - C_t}{C_0} \times 100 \quad (1)$$

The amount of the dye adsorbed onto the adsorbent,  $q_t$  (mg g<sup>-1</sup>), was determined in terms of the change in dye concentration before and after adsorption according to the following equation [47]:

$$q_t = \frac{(C_0 - C_t)V}{w} \quad (2)$$

where  $q_t$  is the amount of dye adsorbed per unit weight of adsorbent at any time  $t$  (mg g<sup>-1</sup>);  $C_0$  and  $C_t$  are the initial and liquid-phase concentrations of the dye solution at any time  $t$  (mg L<sup>-1</sup>), respectively;  $V$  is the volume of the solution (L); and  $w$  is the weight of the sorbent used (g). When  $t$  is equal to the equilibrium agitation time (i.e.,  $C_t = C_e$ ,  $q_t = q_e$ ), then the amount of dye adsorbed at equilibrium,  $q_e$ , (mg g<sup>-1</sup>) is calculated using Eq. (2).

## 2.4. Central composite design (CCD) and optimization of parameters

As mentioned before, a good selection of design and optimization models makes possible to investigate the influences of important variables during the empirical tests simultaneously [48]. In this work, central composite design (CCD) was applied to study the significance of individual and synergetic effects of five variables including initial MB concentration, initial MG concentration, pH, sonication time and adsorbent dosage on two responses; removal percentage of MB ( $R_1$ ) and removal percentage of MG ( $R_2$ ). All experiments were designed using Design-Expert statistical software package 7.0 leading to 32 runs for half-fractional CCD mode (Table 2).



**Table 2**

CCD is basically presented by three operations consisting  $2n$  axial runs,  $2^n$  factorial points and  $N_c$  central points where  $n$  is the number of factors. In the present study CCD is designed based on carrying out 16 factorial points (half-fractional mode), 10 axial points and 4 replicates at the center point (32 experiments). As shown in Table 2, The independent variables were coded based on  $(-1,+1)$  interval indicating the low and high levels, respectively. Alpha ( $\alpha$ ) represents the distance of the axial from center point, which is rotatable and strongly depends on the number of factorial points. The experimental sequence was randomized to minimize the effects of the uncontrolled factors [49,50]. Thereafter, response surface methodology (RSM), a modeling step followed by optimal region determination, was used to improve and optimize the processes besides for estimation and prediction the mathematical relationship between five independent parameters. The related equation can be written by the second order polynomial model [43]:

$$y = \beta_0 + \sum_{i=1}^5 \beta_i X_i + \sum_{i=1}^5 \sum_{j=1}^5 \beta_{ij} X_i X_j + \sum_{i=1}^5 \beta_{ii} X_i^2 \quad (3)$$

Where,  $y$  is the approximated removal percentage as the response;  $X_i$  is showing the independent variables (initial dye concentration, pH, sonication time and adsorbent dosage) determined for each experimental run. The parameter  $\beta_0$  is the model constant;  $\beta_i$  is the linear coefficient;  $\beta_{ii}$  are the quadratic coefficients and  $\beta_{ij}$  are the cross-product coefficients [49]. According to the analysis of variance (ANOVA), the validity of the response surface model was distinguished by measuring the regression coefficients ( $R^2$ ) and lack of fit (LOF). Moreover the most effective parameters were determined on the basis of  $p$ - and  $F$ -values. On the other hand, by plotting the tridimensional graphs of responses ( $R\%$ ) versus the significant parameters, the best operating conditions of dye adsorption was also found graphically.

### **3. Results and Discussion**

### 3.1. Characterization of MIL-68(Al)

Characteristic functional groups of the synthesized MOF were proofed by FT-IR study. The spectra graph indicated the carboxylate groups ( $\nu_{\text{C=O}}$ ) of the MIL- 68(Al) (intense signals at the wavenumber  $1598\text{ cm}^{-1}$  and  $1390\text{ cm}^{-1}$ ),  $\text{U}_2$ -hydroxo groups of the corner-sharing octahedral  $\text{AlO}_4(\text{OH})_2$  (the signal at  $863\text{ cm}^{-1}$ ) and DMF solvent (the peak appeared at  $1656\text{ cm}^{-1}$ ) trapped in the structure. However, the spectrum is in accordance with previous reports [41].

Fig.1.

According to the Fig.2, SEM photographs of the as-synthesized MIL-68 (Al) show the needlelike crystals of MOF with different lengths. The average thickness of each rod is about 20-30 nm.

Fig.2

Based on the XRD pattern (Fig.3), the crystalline structure of MIL-68, which is orthorhombic with a double cell volume was confirmed by comparison with literature [51,52].

Fig.3

BET analysis and some textural properties of the prepared MIL-68(Al) are given in Table3. The BET and Langmuir surface area was measured as  $976$  and  $1484\text{ m}^2/\text{g}$  of synthesized adsorbent respectively. This large surface area and total pore volume favors the suitability of the MOF to remove large amount of dyes very fast using small amount of the adsorbent.

Table 3

The total pore volume ( $V_{\text{Total}}$ ) evaluated by the liquid  $\text{N}_2$  volume at relative pressure of 0.983 was about  $0.70\text{ cm}^3/\text{g}$ . As shown in Fig.4, the synthesized MOF shows major nitrogen sorption at relative pressures less than 0.25. Therefore, the sample is highly microporous. It is necessary to note that the presence of a small hysteresis loop at high relative pressures indicates the presence of mesopores. Pore size distribution can be observed in Fig.4 (inset).

Desorption average pore width obtained by BET and BJH desorption average pore diameter was evaluated about 2.90 and 5.36 nm respectively.

Fig.4.

### **3.2. Analysis of the simultaneous competitive adsorption in binary solutions**

According to Fig.5, the absorbance spectrum of binary mixture containing 5 mg L<sup>-1</sup> of MG and 5 mg L<sup>-1</sup> MB indicates sever overlap while the maximum wavelength corresponding to each dye in their single solution was acquired at 617 and 666 nm, respectively.

Fig.5.

In order to determine the accurate concentration and monitor the competitive adsorption of these dyes in binary mixture, derivative spectrophotometry approach was used as a great utility for separation and reduction of spectral background interferences without need for prior separation [53]. To this end, the absorbance spectra of MG and MB in single and binary solutions were differentiated. The Savitzky–Golay smoothing procedure was then used to improve the ratio of signal-to-noise. Figs.6 and 7 represent the first and second order derivatives of the studied dyes respectively.

Fig.6.

From Fig. 7(a), the second order derivative spectra makes possible to measure MG concentration at a specific wavelength while MB is present but no contribution of MB in the differentiated spectra of the binary solutions is seen at this wavelength. In a similar way, MB dye can be quantified at a special wavelength while MG is present but indicates zero absorbance (Fig.7(a)). The spectra for the second order derivatives at different initial concentrations of MG and MB dyes are presented in Figs.7(b),(c) and (d).

Fig. 7.

After finding the best wavelength for accurate and repeatable determination of the MG and MB content in binary solution, calibration curves were plotted corresponding to each dye at

the proper wavelength. The concentrations were measured theoretically ( $C_t$ ) and experimentally ( $C_{exp}$ ) and then recoveries (%) and errors (%) were determined using Eqs. (4) and (5) respectively [43, 53]:

$$Recovery(\%) = \frac{C_{exp}}{C_t} \times 100 \quad (4)$$

$$Error(\%) = \frac{C_{exp} - C_t}{C_t} \times 100 \quad (5)$$

To check the accuracy of the second-order derivative spectrophotometric method for measurement of target dyes concentration in binary solution, the recovery tests were performed. For this purpose, the binary solutions of MG and MB with different concentrations of each component were prepared. As pointed out before, the concentration of each dye in binary solution was estimated at a given wavelength of the corresponding dye resulted from second order derivative spectra. It should be noted that according to the best of our knowledge the wavelengths reported previously for simultaneous determination of MG and MB dyes concentration were 506.1 and 602.5 nm respectively [53]. However, in this work we tried to analyse the recovery studies with more than one wavelength for each dye in order to find the best wavelength at which the higher recovery values are obtained with minimum error. According to Fig.7(a), the second order derivative spectra of MB is zero at the wavelengths of 618, 506, 620 and 594 nm while MG and their binary solution show clearly non-zero signals. Therefore each of these points could be regarded as the possible optimum wavelength for subsequent analysis of MG dye. The calibration curves were depicted at these selected wavelengths and were used for MG quantification. The values of correlation coefficient ( $R^2$ ) was used to justify the efficiency and suitability of each wavelength. The similar way was done for MB dye and the wavelengths of 598, 638, 692 and 696 nm were considered for further analysis. Table 4 represents the equations and  $R^2$  values obtained for each wavelength. As can be seen, the higher determination coefficient at

692 nm confirms the suitability of this wavelength for calculation of MB concentration. On the other hand, the highest  $R^2$  value was achieved at 594 nm for determination of MG concentration, indicating its priority for simultaneous studies of these two dyes. Therefore, next studies were performed at the selected wavelengths of 692 and 594 nm for MB and MG dyes, respectively.

**Table 4**

The data obtained from the recovery studies at these wavelengths are presented in Supplementary content (Table S5). It is obvious that high and reasonable recovery and low error between the theoretical ( $C_t$ ) and measured concentrations ( $C_{exp}$ ) confirmed the applicability of this method for simultaneous analysis of MG and MB in binary mixtures.

### **3.3. Central composite design under response surface methodology**

As mentioned above, the influence of five independent factors (pH (A), contact time (B), adsorbent dosage (C), MB concentration (D) and MG concentration (E) at three levels (low, central and high) with coded values (-1, 0, +1) and the star points of +2 and -2 for  $+\alpha$  and  $-\alpha$ , respectively was investigated. The general design together with the responses are presented in Table 2. The main, interaction and quadratic effects of variables were then determined using analysis of variance (ANOVA) and the corresponding data for each dye was displayed in Tables 6 and 7. According to the literature, the p-value less than 0.05 for each factor in ANOVA table means that the significance of the related factor is at 95% confidence level. F-test was also applied for evaluation the statistical significance of the variables in the polynomial equation within 95% confidence interval [50].

**Table 6**

From Table 6, it is clear that the factors A, C, D, E, AB, AD, AE, BD, CD, CE,  $A^2$ ,  $C^2$ ,  $D^2$  and  $E^2$  with very low of p-values ( $<0.0001$ ) are significant for MB uptake. However, in the case of MG

(Table 7) the factors A, B, C, D, E, AB, BC, BE, CE, DE, A<sup>2</sup> and D<sup>2</sup> had the most impact on removal percentage of this dye within 95% confidence interval. On the other hand, the quadratic model in both tables is significant (with p < 0.05) indicating the high contribution of the selected model for explanation the adsorption behavior. The lack of fit (LOF) F-value that is relative to the pure error is not significant (2.21 for MB and 4.88 for MG).

**Table 7**

Therefore the suitability of the model for well-fitting the experimental data was concluded. The “Predicted R<sup>2</sup>” (0.907 for MG and 0.942 for MB) is in reasonable agreement with their “Adjusted R<sup>2</sup>” (0.988 for MG and 0.991 for MB) as well as the coefficients of determination (R<sup>2</sup>: 0.995 for MG and R<sup>2</sup>: 0.997 for MB). These values reveal a good correlation and relationship between the experimental or actual data and those calculated from equations. The linear plots of experimental values of removal percentage versus predicted ones, which confirmed these explanations are shown in Supplementary content (Fig.S8).

The final semi-empirical models in terms of significant factors for predicting the removal percentage of MB (R<sub>1</sub>) and MG (R<sub>2</sub>) in binary solution were expressed as following equations respectively:

$$R_1 = +96.28 + 1.88A + 0.21B + 13.52C - 6.60D - 2.22E - 2.51AB - 2.14AC + 3.99AD + 2.88AE - 1.84 \quad (6)$$

$$2.80BD - 2.00BE + 6.04CD + 2.62CE + 0.22DE - 3.48A^2 - 0.79B^2 - 5.89C^2 - 2.00D^2 - 1.65E^2$$

$$R_2 = +77.87 + 3.68A + 4.50B + 12.05C - 17.25D - 3.29E - 4.70AB + 1.09AC + 2.01AD - 0.98AE - \quad (7)$$

$$5.61BC + 1.94BD + 3.61BE + 1.63CD + 3.98CE + 4.63DE - 7.38A^2 - 1.44B^2 - 1.03C^2 - 3.07D^2$$

### 3.4. Response surface methodology and Optimization process

After finding the critical effects, three-dimensional (3D) surface plot of the each response was analyzed using response surface methodology to illustrate the effect of each pair of factors involved in dyes uptake process (Fig. 9a–j). As shown in Figs. 9a, b, i and j, higher removal percentage was occurred at lower dye concentrations and higher adsorbent dosage. As the dyes concentration was increased, the saturation rate increased and the more adsorption sites were being covered [9]. On the other hand, at higher adsorbent dosage, more active adsorption sites are available leading to increase the more number of dye molecules interact with the adsorbent.

According to Figs. 9e and f, removal yield of MB and MG cationic dyes was improved at greater pH which is due to the more negatively charge of the surface at greater values of pH. This phenomenon favors the interaction of dye molecules with the surface through electrostatic attraction. However, as mentioned in the literature other processes like  $\pi$  - $\pi$  stacking interaction and/or hydrophobic interactions may also explain the adsorption mechanism of these dyes on the MOF [14,39].

Figs. 9 c, f, g and h demonstrated the adsorption rate is very rapid and unlike MG, the time factor is not an effective parameter for MB uptake. The removal percentage reaches equilibrium very fast. This event may be attributed to the high available surface area and active sites of the MIL-68(Al) as a promising sorbent. However, the outstanding role of ultrasonic power on improvement of the mass transfer process, amplifying the affinity between adsorbate and adsorbent and accelerating the chemical process cannot be ignored [50].

**Fig. 9.**

The optimization was performed using response surface methodology and the optimal values of pH, ultrasonic time, adsorbent dosage, initial concentration of MB and initial concentration of MG

with desirability function of 1.000 were obtained to be 7.78, 5.0 min, 0.0055 g, 22 mg L<sup>-1</sup> and 12 mg L<sup>-1</sup> respectively.

### 3.5. Adsorption equilibrium study

In order to describe the interaction between the adsorbates and the MIL-68(Al), equilibrium adsorption isotherm models such as, Langmuir, Freundlich and Tempkin models were fitted to analyze the equilibrium data under optimum conditions (pH 7.78, contact time: 5 min, adsorbent dosage: 0.0055 g, MB concentration: 22-600 mg L<sup>-1</sup> and MG concentration: 15-60 mg L<sup>-1</sup>). All experiments were done by 25mL of dye solution at various initial dye concentrations. The linear form of the corresponding isotherm equations followed by their constant parameters and the correlation coefficient ( $R^2$ ) for each model are listed in Table 8. All the model constants were estimated from the slopes and intercepts of respective model equations [37, 54,55].

**Table 8**

According to Langmuir isotherm model (see Table 8), the values of  $K_L$  (the Langmuir adsorption constant, L mg<sup>-1</sup>) and  $q_m$  (theoretical maximum monolayer adsorption capacity (mg g<sup>-1</sup>)) were calculated from the intercept and slope of the plot of  $C_e/q_e$  vs.  $C_e$ , respectively [40]. This model assumes that the adsorption process takes place on completely homogeneous adsorption sites, with each molecule possessing constant sorption activation energy [10]. In Freundlich isotherm model based on the heterogeneous surface energy, a multilayer adsorption occurs and the heat of adsorption is not uniform between the adsorbate molecules [37]. From the Freundlich equation,  $K_F$  (the Freundlich coefficient corresponding to adsorption capacity, ((mg g<sup>-1</sup>)/(mg L<sup>-1</sup>)<sup>1/n</sup>) and 1/n (an exponential coefficient indicative the adsorption intensity) can be determined from the linear plot of  $\ln q_e$  vs.  $\ln C_e$ , respectively. The equilibrium data were also analyzed by Tempkin model to further elucidate the simultaneous adsorption behavior of MB and MG dyes onto MIL-68(Al). Following plotting the  $q_e$  versus  $\ln C_e$ , based on the slope and intercept value of line, the heat of the adsorption



( $B_1 = \frac{RT}{b}$ , J mol<sup>-1</sup>) and  $K_T$  (the equilibrium binding constant corresponding to the maximum binding energy, L mol<sup>-1</sup>) were obtained respectively. In this equation, T is the absolute temperature (K) and R is the universal gas constant (8.314 J mol<sup>-1</sup> K<sup>-1</sup>) [55]. As shown in Table 8, in comparison with freundlich model, the high correlation coefficient of Langmuir isotherm (0.9981 and 0.9993 for MB and MG, respectively) confirms the closeness of the adsorption model to this isotherm. Freundlich isotherm model did not fit well with the experimental data indicating its inapplicability for interpretation of the data. Notably, MIL-68(Al) revealed an enormous potential to adsorb both dyes with maximum monolayer adsorption capacity of 666.67 and 153.85 mg g<sup>-1</sup> for MB and MG respectively. The reported statistics in the current study are far more than the commercial activated carbon (9.8–238 mg g<sup>-1</sup>) [56,57] and many other materials which have been used as adsorbents for MB or MG uptake [49,54,58,59]. The high dye adsorption capacity of MIL-68(Al) may be attributed to the 3D porous framework of this MOF and its high specific surface area.

### 3.6. Adsorption kinetics study

To understand the rate and adsorption mechanism involved in the removal of MG/MG by the synthesized MOF, the experimental kinetic data were analyzed through the conventional kinetic models including pseudo-first order, pseudo-second order and Elovich equations. The linear form of the equation corresponding to each kinetic model and their relative parameters that were calculated are summarized in Table 9.

**Table 9**

The results showed that the sorption kinetics is described by pseudo second order model very well. The higher values of the regression correlation coefficients of pseudo-second-order kinetic model ( $R^2 = 1.0$ ) and closeness of the experimental and theoretical adsorption capacity ( $q_e$ ) values verified that the chemisorption was the rate-controlling step over the whole adsorption process. On

the other hand, the Elovich equation as another rate equation showed the correlation coefficient higher than 0.94, which not only indicated the suitability of this model for evaluation of the adsorption nature but also confirmed that the rate-limiting step was very close to chemisorption [60,61].

### 3.7. Desorption and regeneration studies

Reusability of an adsorbent is key parameter for commercial feasibility. In this study, to understand the adsorption mechanism more effectively and to recover the depleted adsorbent, desorption and regeneration processes of dye-loaded MIL-68(Al) were carried out using hydrochloric acid aqueous solution (0.01 M), sodium chloride aqueous solution (0.01 M) and methanol solvent. Compared with the other two chemicals, methanol was the best strippant for attached dyes on the adsorbent, which implies that the adsorption should be directed by chemical bonds between dye molecules and surface of the adsorbent. Therefore, the other regeneration experiments were done using methanol. Typically, 0.055 g of MIL-68(Al) was added to 25 mL of dye solution with concentration of 220 mg L<sup>-1</sup> MB and 120 mg L<sup>-1</sup> MG under ultrasonic radiation for 5 min. After centrifugal separation, the dye-loaded adsorbent was added to 15 mL of methanol and was maintained in ultrasonic bath for 7 min. This desorption process was performed at least four times until no dye can be detected. The adsorbent was then collected, dried under vacuum at 463 K overnight and reused. The regeneration efficiency (RE%) as a criterion for evaluation the reusability of the dye uploaded MOF was calculated by the following equation [62].

$$RE (\%) = \frac{q_r}{q_e} \times 100 \quad (8)$$

Where  $q_r$  and  $q_e$  are the adsorption capacity of the regenerated and virgin adsorbent respectively. According to Table 10 even though the adsorption percentage decrease gradually after each cycle, the removal percentage and regeneration efficiency of the sorbent are still significant (higher than 78% and 85% respectively). The reduction of dyes uptake efficiency may be due to the incomplete

removal of the dye molecules from the adsorbents, resulting in the decrease of the surface area and non-availability of the adsorptive active sites. It can be claimed that a certain proportion of the dyes are strongly retained in the adsorbent cannot be removed by a simple chemical treatment. However, the reported statistics demonstrated the acceptable reusability of the prepared MOF and its remarkable potential for dye removal even after three adsorption – desorption cycles.

**Table 10**

### **3.8. Effect of ionic strength**

In fact, there are several salts and metal ions in dye contaminated or industrial wastewaters, which can act as interfering agent, strengthen or weaken the dye adsorption process. Salts are one of the most popular materials in real samples lead to enhance the ionic strength that subsequently affects the efficiency of dye adsorption. For this reason in the current research, NaCl and KCl solutions with different concentrations of 0.01, 0.05 and 0.1 mol L<sup>-1</sup> were chosen to investigate the effect of ionic strength on the adsorption of MB and MG onto the MIL-68(Al) under optimum condition. According to our results (Table 11), the adsorption percentage decreased gradually as the concentration of NaCl or KCl further increased from 0.01 to 0.1 mol L<sup>-1</sup>. This phenomenon may be described by the competition occurred between the K<sup>+</sup> or Na<sup>+</sup> cations from the salt and cationic dyes for occupying active sites of the adsorbent. Meanwhile, KCl had more negative effect on the adsorption efficiency due to the larger ionic radius of K<sup>+</sup> cation than Na<sup>+</sup>. These results suggested that electrostatic interaction is one of the possible mechanisms for the simultaneous removal of MB or MG on MIL-68(Al) [60, 63].

**Table 11**

### **3.9. Comparison with other adsorbents and methods**

A comparison between the performance of the proposed adsorbent and method with some adsorbents and methods is listed in Table 12. It is important to imply that, the values reported for “q (mg g<sup>-1</sup>)” in Table 12 are mostly attributed to the maximum adsorption capacities of the adsorbents

just in the single dye component system (a solution containing MB or MG dye). It is supposed that in comparison with the multi-component solutions, a larger amount of the desired dye could be removed by the adsorbent in single-component solution under the same condition. However, the maximum adsorption capacities obtained in this work for binary dye mixtures were still superior to many other adsorbents proposed before for single dye uptake.

It is obvious that MIL-68(Al) is preferable to those similar reports in terms of contact time and adsorption capacity especially for MB removal. The strongly adsorption of MG and MB on the surface of MIL-68(Al) may be due to the large surface area and more active adsorption sites of the proposed MOF as well as surface complexation and electrostatic interactions between cationic adsorbates and the organic-inorganic adsorbent.

**Table 12**

#### **4. Conclusions**

MIL-68(Al) was synthesized by solvothermal method, which was reported before. Regarding to the extremely importance of dye removal from multi-component systems, the desired MOF was used as an adsorbent in the simultaneous adsorptive removal of MB and MG cationic dyes from aqueous solution for the first time. These studied dyes exhibited severe spectra overlapping. Therefore, the utilization of an efficient method in order to overcome this problem was unavoidable. In the current research, second-order derivative spectrophotometric analysis method was applied to analyze the concentration of each dye in binary mixtures with high accuracy. Because of its specific characteristics including high surface area, suitable pore size, nearly homogenous pore distribution and good thermal stability, MIL-68(Al) revealed excellent adsorption properties under mild reaction conditions. Central Composite Design (CCD) under Response surface methodology (RSM) approach was proposed in order to investigate and optimize the influences of variables on the removal percentages of the dyes. The optimum value corresponding to each parameter at which the removal percentages of the dyes were maximum was found to be 12 mg L<sup>-1</sup>, 22 mg L<sup>-1</sup>, 7.78, 0.0055

g and 5 min for initial MG concentration, initial MB concentration, pH of the solution, adsorbent dosage and ultrasonic contact time respectively. The resulted statistics confirmed that satisfactory dye uptake is completely possible only by using small amount of the MOF in very short time. The investigation was carried out in view of the adsorption isotherm, kinetics, and regeneration of the sorbent. Among the conventional isotherm equations such as Langmuir, Freundlich and Tempkin, the first model was the best option for description the equilibrium data. The kinetic studies was done by different models in which pseudo-second-order kinetic equation posed a better agreement with the adsorption process. From the data obtained by reusability tests the removal percentage and regeneration efficiency of the sorbent were still significant even after three adsorption-desorption cycles, demonstrating the good reusability of the prepared MOF. Ionic strength of the solution was increased by addition the specific amounts of NaCl or KCl to the binary mixture of dyes and the findings showed that the adsorption percentage decreased gradually as the concentration of NaCl or KCl increased verifying the negative and comparative effect of the soluble salts on dye removal process. The performance of the presented MOF and method is comparable and superior to many other materials have been used for dye uptake in the literature.

## **Acknowledgements**

The financial support of this study by Iran University of Science and Technology and Nano Technology Initiative Council are gratefully acknowledged. The author acknowledges financial support from the Iran National Science Foundation (INSF).

## References

- [1] Maryam Shanehsaz, Shahram Seidi, Yousefali Ghorbani, Seyed Mohammad Reza Shoja, Shohre Rouhani, *Spectrochim. Acta A.* 149 (2015) 481–486.
- [2] Q. Zhou, Q. Gao, W. Luo, C. Yan, Z. Ji, P. Duan, *Colloid. Surface A.* 470 (2015) 248–257.
- [3] L.S. Silva, L.C.B. Lima, F.C. Silva, J.M.E. Matos, M.R.M.C. Santos, L.S.S. Júnior, K. S. Sousa, E.C.d.S. Filho, *Chem. Eng. J.* 218 (2013) 89–98.
- [4] D.T. Sponza, Toxicity studies in a chemical dye production industry in Turkey, *J. Hazard. Mater.* 138 (2006) 438–447.
- [5] V.K. Gupta, Alok Mittal, Lisha Krishnan, Vibha Gajbe, *Sep Purif Technol.* 40 (2004) 87–96.
- [6] M. Makeswari, T. Santhi, *Journal of Water Resource and Protection*, 5 (2013) 222–238.
- [7] H. Aliyan, R. Fazaeli, R. Jalilian, *Appl. Surf. Sci.* 276 (2013) 147–153.
- [8] B.R. Ganapuram, M. Alle, R. Dadigala, A. Dasari, V. Maragoni, V. Guttena, *Int Nano Lett.* (2015) DOI 10.1007/s40089-015-0158-3.
- [9] R. Ansari, M. S. Tehrani, A. Mohammad-khah, J. Wood. *Chem. Technol.* 32 (2012) 198–209.
- [10] R. L. Liu, Y. Liu, X. Y. Zhou, Z. Q. Zhang, J. Zhang, F. Q. Dang, *Bioresource. Technol.* 154 (2014) 138–147.
- [11] H. Jianga, P. Chen, S. Luo, X. Tu, Q. Cao, M. Shu, *Appl. Surf. Sci.* 284 (2013) 942–949.
- [12] Y. Feng, H. Zhou, G. Liu, J. Qiao, J. Wang, H. Lu, L. Yang, Y. Wu, *Bioresource. Technol.* 125 (2012) 38–144.
- [13] A. Aygun, S. Y. Karakas, I. Duman, *Micropor. Mesopor. Mater.* 66 (2003) 189–195.
- [14] Y. Li, Q. Du, T. Liu, X. Peng, J. Wang, J. Sun, Y. Wang, S. Wu, Z. Wang, Y. Xia, L. Xia, *Chem. Eng. Res. Des.* 91 (2013) 361–368.
- [15] G. Crini, *Dyes. Pigments.* 77 (2008) 415–426.
- [16] V. K. Gupta, D. Pathania, N.C. Kothiyal, G. Sharma, *J. Mol. Liq.* 190 (2014) 139–145.
- [17] B.S. Inbaraj, B.H. Chen, *Bioresource. Technol.* 102 (2011) 8868–8876.
- [18] R. Kumar, V.K. Garg, R. Gupta, *Dyes. Pigments.* 62 (2004) 1–10.
- [19] G. Crini, *Bioresource. Technol.* 97 (2006) 1061–1085.
- [20] M. Rafatullah, O. Sulaiman, R. Hashim, A. Ahmad, *J. Hazard. Mater.* 177 (2010) 70–80.
- [21] L. Fan, C. Luo, M. Sun, X. Li, F. Lu, H. Qiu, *Bioresource. Technol.* 114 (2012) 703–706.
- [22] V. K. Gupta, A. Nayak, *Chem. Eng. J.* 180 (2012) 81–90.
- [23] Y. Yao, S. Miao, S. Liu, L. P. Ma, H. Sun, S. Wang, *Chem. Eng. J.* 184 (2012) 326–332.
- [24] D. Wang, L. Liu, X. Jiang, J. Yu, X. Chen, *Colloid Surface A.* 466 (2015) 166–173.
- [25] S. T. Yang, S. Chen, Y. Chang, A. Cao, Y. Liu, H. Wang, *J. Colloid. Interf. Sci.* 359 (2011) 24–29.
- [26] E. C. D. Oliveira, C. T. G. V. M. T. Pires, H. O. Pastore, *J. Braz. Chem. Soc.* 17 (2006) 16–29.
- [27] O. Ozdemir, B. Armagan, M. Turan, M. S. Celik, *Dyes. Pigments.* 62 (2004) 49–60.
- [28] N. A. Khan, Z. Hasan, S. H. Jhung, *J. Hazard. Mater.* 244–245 (2013) 444–456.

- [29] S. Lin, Z. Song, G. Che, A. Ren, P. Li, C. Liu, J. Zhang, *Micropo. Mesopor. Mat.* 193 (2014) 27–34.
- [30] Md. R. Awual, Md. M. Hasan, T. Ihara, T. Yaita, *Micropo. Mesopor. Mat.* 197 (2014) 331–338.
- [31] Md. R. Awual, T. Yaita, S.A.El-Safty, H. Shiwaku, Y. Okamot, S. Suzuki, *Chem. Eng. J.* 222 (2013) 172–179.
- [32] Md. R. Awual, T. Yaita, S. A. El-Safty, H. Shiwaku, S. Suzuki, Y. Okamoto, *Chem. Eng. J.* 221 (2013) 322–330.
- [33] Md. R. Awual, Md. M. Hasan, *Sensor Actuat B-Chem.* 202 (2014) 395–403.
- [34] B. V. d. Voorde, B. Bueken, J. Denayer, D. D. Vos, *Chem. Soc. Rev.* 43 (2014) 5766–5788.
- [35] J. Y. Cheng, P. Wang, J. P. Ma, Q. K. Liu, Y. B. Dong, *Chem. Commun.* 50 (2014) 13672–13675.
- [36] S. H. Huo, X. P. Yan, *Analyst.* 137 (2012) 3445–3451.
- [37] C. Chen, M. Zhang, Q. Guan, W. Li, *Chem. Eng. J.* 183 (2012) 60– 67.
- [38] J. D. Xiao, L. G. Qiu, X. Jiang, Y. J. Zhu, S. Ye, X. Jiang, *Carbon.* 59 (2013) 372–382.
- [39] S. H. Huo, X. P. Yan, *J. Mater. Chem.* 22 (2012) 7449–7455.
- [40] L. Jin, X. Qian, J. Wanga, H. Aslan, M. Dong, *J. Colloid. Interf. Sci.* 453 (2015) 270–275.
- [41] Q. Yang, S. Vaesen, M. Vishnuvarthan, F. Ragon, C. Serre, A. Vimont, M. Daturi, G. Weireld, G. Maurin, *J. Mater. Chem.* 22 (2012) 10210–10220.
- [42] S. Hajati, M. Ghaedi, B. Barazesh, F. Karimi, R. Sahraei, A. Daneshfar, A. Asghari, *J. Ind. Eng. Chem.* 20 (2014) 2421–2427.
- [43] S. Hajati , M. Ghaedi , F. Karimi , B. Barazesh , R. Sahraei , A. Daneshfar, *J. Ind. Eng. Chem.* 20 (2014) 564–571.
- [44] M. R. Sohrabi, S. Amiri, H. R. F. Masoumi, M. Moghri, *J. Ind. Eng. Chem.* 20 (2014) 2535–2542.
- [45] S. Honary, P. Ebrahimi, H. Asgari-rad, F. Mohamadpour, *Int. J. Nanosci. Nanotechnol*, 10 (2014) 257–261.
- [46] M. Roosta, M. Ghaedi, M. Mohammadi, *Powder Technol.* 267 (2014) 134–144.
- [47] X. Li, L. Zheng, L. Huang, O. Zheng, Z. Lin, L. Guo, B. Qiu, G. Chen, *J. Appl. Polym. Sci.* 129 (2013) 2857–2864.
- [48] M. Roosta, M. Ghaedi, A. Daneshfar, S. Darafarin, R. Sahraei, M.K. Purkait, *Ultrason. Sonochem* 21 (2014) 1441–1450.
- [49] M. Ghaedi, H. Mazaheri, S. Khodadoust, S. Hajati, M.K. Purkait, *Spectrochim. Acta A.* 135 (2015) 479–490.
- [50] M. Roosta, M. Ghaedi, A. Daneshfar, R. Sahraei, A. Asghari, *Ultrason. Sonochem.* 21 (2014) 242–252.
- [51] B. Seoane, V. Sebastián, C. Téllez and J. Coronas, *Cryst Eng Comm.* 15 (2013) 9483–9489.
- [52] T. Han, Y. Xiao, M. Tong, H. Huang, D. Liu, L. Wang, C. Zhong, *Chem. Eng. J.* 275 (2015) 134–141.
- [53] M. Ghaedi, S. Hajati, M. Zare, M. Zare, S. Y. S. Jaber, *RSC Adv.* 5 (2015) 38939–38947.
- [54] E. Haque, J. W. Jun, S. H. Jung, *J. Hazard. Mater.* 185 (2011) 507–511.

- [55] Z. Wu, H. Zhong, X. Yuan, H. Wang, L. Wang, X. Chen, G. Zeng, Y. Wu, *water. res.* 67 (2014) 330-344.
- [56] B. Bestani, N. Benderdouche, B. Benstaali, M. Belhakem, A. Addou, *Bioresource. Technol.* 99 (2008) 8441–8444.
- [57] K. Marungrueng, P. Pavasant, *Bioresource. Technol.* 98 (2007) 1567–1572.
- [58] M. Ghaedi, S. N. Kokhdan, *Spectrochim. Acta A.* 136 (2015) 141-148.
- [59] H. Zhang, Y. Tang, X. Liu, Z. Ke, X. Su, D. Cai, X. Wang, Y. Liu, Q. Huang, Z. Yu, *Desalination.* 274 (2011) 97–104.
- [60] L. Xie, D. Liu, H. Huang, Q. Yang, C. Zhong, *Chem. Eng. J.* 246 (2014) 142–149.
- [61] P. Sharma, B. K. Saikia, M. R. Das, *Colloid Surface A.* 457 (2014) 125–133.
- [62] R. Ansari, M. S. Tehrani, M.B. Keivani, *J. Wood Chem. Technol.* 33 (2013) 19–32.
- [63] Q. D. Qin, J. Ma, K. Liu, *J Colloid. Interf. Sci.* 315 (2007) 80–86.
- [64] C. S. Ozdemir, *Physicochem. Probl. Miner. Process.* 48 (2012) 441–454.
- [65] L. Xiong, Y. Yang, J. Mai, W. Sun, C. Zhang, D. Wei, Q. Chen, J. Ni, *Chem. Eng. J.* 156 (2010) 313–320.
- [66] S. Shaibu , F. Adekola , H. Adegoke , O. Ayanda, *Materials.* 7 (2014) 4493-4507.
- [67] R. Han, J. Zhang, P. Han, Y. Wang, Z. Zhao, M. Tang, *Chem. Eng. J.* 145 (2009) 496–504.
- [68] M. Ghaedi, Sh. Heidarpour, S. N. Kokhdan, R. Sahraie, A. Daneshfar, B. Brazesh, *Powder Technol.* 228 (2012) 18–25.
- [69] M. Ghaedi, M. Pakniat, Z. Mahmoudi, S. Hajati, R. Sahraei, A. Daneshfar, *Spectrochim. Acta A.* 123 (2014) 402- 409.
- [70] C. Li, Z. Xiong, J. Zhang, C. Wu, *J. Chem. Eng. Data.* 60 (2015) 3414-3422.
- [71] S. Hajati, M. Ghaedi, S. Yaghoubi, *J. Ind. Eng. Chem.* 21 (2015) 760-767.
- [72] M. Roosta, M. Ghaedi, N. Shokri, A. Daneshfar, R. Sahraei, A. Asghari, *Spectrochim. Acta A.* 118 (2014) 55–65.
- [73] M. Ghaedi, A. Ansari, M. H. Habibi, A.R. Asghari, *J. Ind. Eng. Chem.* 20 (2014) 17-28.
- [74] Z. Bekci, C. O' zveri, Y. Seki, K. Yurdakoc, *J. Hazard. Mater.* 154 (2008) 254-261.
- [75] M. Setareh Derakhshan, O. Moradi, *J. Ind. Eng. Chem.* 20 (2014) 3186–3194.
- [76] Uma, S. Banerjee, Y. C. Sharma, *J. Ind. Eng. Chem.* 19 (2013) 1099–1105.
- [77] M. Rajabi, B. Mirza, K. Mahanpoor, M. Mirjalili, F. Najafi, O. Moradi, H. R. Sadegh, R. Shahryari-ghoshekandi, M. Asif, I. Tyagi, S. Agarwal, V. K. Gupta, *J. Ind. Eng. Chem.* (2015) [10.1016/j.jiec.2015.11.001](https://doi.org/10.1016/j.jiec.2015.11.001).



## Figure captions

**Fig.1.** FT- IR spectra of MIL-68(Al) sample

**Fig.2.** SEM images of the as-prepared MIL-68 (Al)

**Fig. 3.** XRD diffraction pattern of synthesized MIL-68(Al)

**Fig.4.** N<sub>2</sub> adsorption/desorption isotherm at 77 K and BJH pore size distributions (inset) for synthesized MIL-68(Al)

**Fig.5.** Absorption spectra of MG and MB in single and binary solutions (initial dye concentration of 5 mg L<sup>-1</sup> for each dye).

**Fig.6.** First order derivative spectra of MG and MB in single and binary solutions (initial dye concentration of 5 mg L<sup>-1</sup> for each dye).

**Fig.7.** (a) Second order derivative spectra of MG and MB in single and binary Solutions (initial dye concentration of 5mg L<sup>-1</sup>), (b) Second order derivative spectra of MG and MB in binary solutions with different initial MB and MG concentration(c) Second order derivative spectra of MG and MB in binary solutions with constant MB concentration and (d) Second order derivative spectra of MG and MB in binary solutions with constant MG concentration

**Fig.S8.** The experimental (actual) data versus the predicted data for removal of (a) MB (b) MG in binary solution

**Fig.9.** Response surfaces for the CCD: (a) E-C (MB) ; (b) D-C MB); (c) D-B (MB); (d) E-A (MB); (e) B-A (MB) (f) B-A (MG); (g) C-B (MG); (h) E-B (MG); (i) E-C (MG) and (j) E-D (MG)

## Table Captions

**Table S1** Some of the most important properties of Methylene Blue and Malachite Green dyes

**Table 2** Experimental factors, levels and responses for binary dye solutions according to the central composite design.

**Table 3** BET analysis and textural properties of the synthesized MIL-68(Al)

**Table 4** Calibration curve and corresponding  $R^2$  at each wavelength obtained by SODS method for MB and MG in single dye solution

**Table S5** Recovery and error percentages values obtained by SODS method for MG and MB in their binary solution

**Table 6** ANOVA for response surface quadratic model for MB removal in binary solution

**Table 7** ANOVA for response surface quadratic model for MG removal in binary solution

**Table 8** Adsorption isotherms of MB and MG adsorption onto MIL-68(Al)



**Table 9** Pseudo-first-order, Pseudo-second-order and Elovich kinetics constants of MB and MG adsorption onto MIL-68(Al)

**Table 10** Regeneration process parameters of three adsorption/desorption cycles

**Table 11** The effect of NaCl and KCl salts on adsorption percentage of MIL-68(Al) for MB and MG removal

**Table 12** Comparison for the removal of MB and MG dyes by different adsorbents and methods

**Table S1** Some of the most important properties of Methylene Blue and Malachite Green dyes

Properties	Methylene blue (MB)	Malachite Green (MG)
Color index number	52015	45170
CAS number	61-73-44444	569-64-2
Chemical formula	$C_{16}H_{18}N_3SCl$	$C_{23}H_{25}ClN_2$
Molecular weight ( $g\ mol^{-1}$ )	319.85	364.911
Maximum wavelength ( $\lambda_{max}$ ) (nm)	664	616
Chemical structure and appearance	<div><chem>CN(C)c1ccc2nc3ccc(cc3[n+]([CH3])Cl)sc2c1</chem> </div>	<div><chem>CN(C)c1ccc(cc1)C(=C2C=CC(=[N+]([CH3])Cl)C=C2)c3ccccc3</chem> </div>
Type of dye	Basic blue (Cationic)	Triarylmethane (Cationic)
Use	Redox indicator, coloring paper, cottons and hair colorant	Coloring paper, leather and silk

**Table 2** Experimental factors, levels and responses for binary dye solutions according to the central composite design.

Factors	Levels			Star point	
	Low	Central		$-\alpha$	$+\alpha$
	High (-1)	(0)	(+1)		
(A) pH	6	7.5	9	4.5	10.5
(B) Time	4	6	8	2	10
(C) Adsorbent dosage	2.5	4	5.5	1	7
(D) MB Concentration	20	30	40	10	50
(E) MG Concentration	10	15	20	5	25

Runs	A	B	C	D	E	R <sub>1</sub>	R <sub>2</sub>
1	6.00	4.00	2.50	20.00	20.00	68.36	45.29
2(c)	7.50	6.00	4.00	30.00	15.00	96.64	77.00
3	9.00	4.00	2.50	20.00	10.00	80.13	84.62
4(c)	7.50	6.00	4.00	30.00	15.00	97.22	79.45
5	6.00	8.00	5.50	40.00	10.00	94.03	50.22
6	9.00	8.00	5.50	40.00	20.00	93.45	73.56
7	9.00	8.00	2.50	20.00	20.00	80.63	67.16
8	7.50	6.00	1.00	30.00	15.00	44.87	49.18
9	6.00	4.00	5.50	20.00	10.00	98.06	94.77
10	6.00	4.00	5.50	40.00	20.00	92.31	54.00
11	10.5	6.00	4.00	30.00	15.00	85.54	55.60
12	9.00	4.00	5.50	40.00	10.00	100.15	71.28
13(c)	7.50	6.00	4.00	30.00	15.00	95.06	79.20
14	7.50	2.00	4.00	30.00	15.00	93.69	61.20
15	9.00	4.00	2.50	40.00	20.00	67.22	25.56
16	7.50	6.00	7.00	30.00	15.00	100.01	96.29
17	6.00	8.00	5.50	20.00	20.00	100.22	93.46
18	7.50	10.0	4.00	30.00	15.00	92.05	80.96
19	4.50	6.00	4.00	30.00	15.00	78.60	39.00
20	6.00	4.00	2.50	40.00	10.00	51.69	18.14
21	9.00	8.00	2.50	40.00	10.00	65.22	45.26
22	6.00	8.00	2.50	40.00	20.00	40.41	49.66
23(c)	7.50	6.00	4.00	30.00	15.00	97.37	77.53
24	7.50	6.00	4.00	10.00	15.00	99.51	100.0
25	7.50	6.00	4.00	30.00	25.00	85.82	68.17
26	9.00	4.00	5.50	20.00	20.00	98.66	95.90
27	7.50	6.00	4.00	50.00	15.00	76.53	29.12
28	9.00	8.00	5.50	20.00	10.00	90.93	88.05
29(c)	7.50	6.00	4.00	30.00	15.00	97.15	76.10
30	6.00	8.00	2.50	20.00	10.00	100.02	90.62
31	7.50	6.00	4.00	30.00	5.00	92.99	88.52
32(c)	7.50	6.00	4.00	30.00	15.00	94.75	77.02

C: center point, R<sub>1</sub>: MB removal%, R<sub>2</sub>: MG removal%

**Table 3** BET analysis and textural properties of the synthesized MIL-68(Al)

Sample	S <sub>BET</sub> (m <sup>2</sup> /g)	S <sub>INT</sub> (m <sup>2</sup> /g)	S <sub>EXT</sub> (m <sup>2</sup> /g)	V <sub>Total</sub> (cm <sup>3</sup> /g)	V <sub>MICRO</sub> (cm <sup>3</sup> /g)
MIL-68(Al)	976	776	200	0.70	0.44

**Table 4** Calibration curve and corresponding R<sup>2</sup> at each wavelength obtained by SODS method for MB and MG in single dye solution

Dye	Wavelength (nm)	Calibration Curve	Correlation Coefficient (R <sup>2</sup> )
MB	598	y = 0.0966x - 0.0794	0.992
	638	y = 0.1263x - 0.0019	0.981
	692	y = 0.0418x + 0.0088	0.995
	696	y = 0.0229x + 0.0038	0.991
MG	618	y = 0.1173x - 0.0057	0.992
	506	y = 0.007x + 0.0014	0.985
	620	y = 0.1159x - 0.0058	0.992
	594	y = 0.090x - 0.012	0.999

**Table S5** Recovery and error percentages values obtained by SODS method for MG and MB in their binary solution

Theoretical (mg L <sup>-1</sup> )		Experimental (mg L <sup>-1</sup> )		Recovery (%)		Error (%)	
C <sub>MB</sub>	C <sub>MG</sub>	C <sub>MB</sub>	C <sub>MG</sub>	MB	MG	MB	MG
40	10	36.85	11.76	92.12	117.6	-7.87	17.6
20	10	19.07	10.01	95.35	100.1	-4.64	0.1
30	25	28.81	25.11	96.07	100.4	-3.93	0.44
20	25	20.75	23.42	103.8	93.68	3.75	-6.32
30	15	29.69	14.80	98.97	98.69	-1.03	-1.33
40	20	35.94	20.68	89.86	103.40	-10.15	3.4
20	20	19.77	20.12	98.86	100.6	-1.15	0.62
50	15	44.36	16.07	88.73	107.13	-11.27	7.13
10	15	10.52	14.47	105.2	96.46	5.20	-3.53
10	10	10.20	9.88	102.0	98.80	2.00	-1.20
15	15	15.33	15.11	102.2	100.73	2.2	0.733

**Table 6** ANOVA for response surface quadratic model for MB removal in binary solution

Source	Sum of Squares	df	Mean Square	F-value	Prob > F
Model	8489.07	20	424.45	189.33	<0.0001
A-pH	85.13	1	85.13	37.97	<0.0001
B-Time	1.01	1	1.01	0.45	0.5162
C-Dosage	4385.35	1	4385.35	1956.09	<0.0001
D-MB concentration	1046.50	1	1046.50	466.79	<0.0001
E-MG concentration	118.37	1	118.37	52.80	<0.0001
AB	100.80	1	100.80	44.96	<0.0001
AC	73.02	1	73.02	32.57	0.0001
AD	255.20	1	255.20	113.83	<0.0001
AE	132.37	1	132.37	59.04	<0.0001
BC	54.02	1	54.02	24.10	0.0005
BD	125.66	1	125.66	56.05	<0.0001
BE	64	1	64	28.55	0.0002
CD	583.95	1	583.95	260.47	<0.0001
CE	109.73	1	109.73	48.94	<0.0001
DE	0.78	1	0.78	0.35	0.5664
A <sup>2</sup>	356.24	1	356.24	158.90	<0.0001
B <sup>2</sup>	18.36	1	18.36	8.19	0.0155
C <sup>2</sup>	1018.89	1	1018.89	454.48	<0.0001
D <sup>2</sup>	117.03	1	117.03	52.20	<0.0001
E <sup>2</sup>	79.97	1	79.97	35.67	<0.0001
Residual	24.66	11	2.24		
Lack of Fit	17.92	6	2.99	2.21	0.2005not significant
Pure Error	6.74	5	1.35		
Cor total	8513.73	31			

 $R^2 = 0.997$ , adjusted  $R^2 = 0.991$ , predicted  $R^2 = 0.942$

**Table 7** ANOVA for response surface quadratic model for MG removal in binary solution

Source	Sum of Squares	df	Mean Square	F-value	Prob > F
Model	15366.67	19	808.77	139.63	<0.0001
A-pH	325.46	1	325.46	56.19	<0.0001
B-Time	485.10	1	485.10	83.75	<0.0001
C-Dosage	3482.45	1	3482.45	601.21	<0.0001
D-MB	7138.05	1	7138.05	1232.32	<0.0001
concentration					
E-MG	260.17	1	260.17	44.92	<0.0001
concentration					
AB	352.88	1	352.88	60.92	<0.0001
AC	18.92	1	18.92	3.27	0.0958
AD	64.40	1	64.40	11.12	0.0059
AE	15.29	1	15.29	2.64	0.1302
BC	504.0	1	504.0	87.01	<0.0001
BD	60.30	1	60.30	10.41	0.0073
BE	208.80	1	208.80	36.05	<0.0001
CD	42.25	1	42.25	7.29	0.0193
CE	252.97	1	252.97	43.67	<0.0001
DE	342.99	1	342.99	59.21	<0.0001
A <sup>2</sup>	1610.75	1	1610.75	278.08	<0.0001
B <sup>2</sup>	61.21	1	61.21	10.57	0.0069
C <sup>2</sup>	31.08	1	31.08	5.37	0.0390
D <sup>2</sup>	278.30	1	278.30	48.05	<0.0001
Residual	69.51	12	5.79		
Lack of Fit	60.63	7	8.66	4.88	0.0500not significant
Pure Error	8.88	5	1.78		
Cor total	15436.18	31			

 $R^2 = 0.995$ , adjusted  $R^2 = 0.988$ , predicted  $R^2 = 0.907$



**Table 8** Adsorption isotherms of MB and MG adsorption onto MIL-68(Al)

Isotherm	Equation	Plot	Parameter	Values of parameters	
				MB	MG
Langmuir	$\frac{c_e}{q_e} = \frac{c_e}{q_m} + \frac{1}{K_L q_m}$	The values of $q_m$ and $K_L$ were calculated respectively from the slope and intercept of the plot of $C_e/q_e$ versus $C_e$	$q_m$	666.67	153.85
			$K_L$	0.081	0.575
			$R^2$	0.9981	0.9993
Freundlich	$\ln q_e = \ln K_F + \frac{1}{n} \ln C_e$	The values of $K_F$ and $n$ were calculated respectively from the intercept and slope of the plot of $\ln q_e$ versus $\ln C_e$	$K_F$	114.99	61.76
			$n$	3.402	3.398
			$R^2$	0.9857	0.8654
Tempkin	$q_e = B_1 \ln K_T + B_1 \ln C_e$	The values of $B_1$ and $K_T$ were calculated from the plot of $q_e$ against $\ln C_e$	$K_T$	2.473	9.468
			$B_1$	90.067	27.51
			$R^2$	0.9911	0.9298

**Table 9** Pseudo-first-order, Pseudo-second-order and Elovich kinetics constants of MB and MG adsorption onto MIL-68(Al)

Model	Equation	Plot	Parameters	Values of parameters	
				MB	MG
first-order	$\log(q_e - q_t) = \log q_{e1} - \frac{k_1}{2.303} t$	the values of $k_1$ and $q_{e1}$ were calculated from the slope and intercept of the plot of $\log(q_e - q_t)$ versus $t$ , respectively	$q_e$ (mg g <sup>-1</sup> )	1.0512	6.175
			$K_1$ (L/min)	0.6630	0.5324
			$R^2$	0.9700	0.9608
second-order	$\frac{t}{q_t} = \frac{1}{k_2 q_{e2}^2} + \frac{1}{q_{e2}} t$	The values of $k_2$ and $q_{e2}$ , were calculated from the intercept and slope of the plot of $t/q_t$ versus $t$ , respectively	$K_2$ (g mg <sup>-1</sup> min <sup>-1</sup> )	-1.2017	0.2895
			$q_{e2}$	96.1540	51.5461
			$R^2$	1.0000	1.0000
Elovich	$q_t = 1/\beta \ln(\alpha\beta) + 1/\beta \ln(t)$	The value of $\beta$ were calculated from the slope of the plot of $q_t$ versus $\ln(t)$	$\beta$	2.9958	1.7559
			$R^2$	0.9852	0.9840
			$q_e$ (exp)	96.6619	51.3777

**Table 10** Regeneration process parameters of three adsorption/desorption cycles

D	Cycle	$q_{c\ exp}$ (mg g <sup>-1</sup> )	% Removal	RE (%)
MB	1	95.88	95.88	-
	2	93.15	93.15	97.15
	3	82.04	82.04	85.56
MG	1	48.75	89.38	-
	2	47.28	86.69	96.99
	3	42.84	78.55	87.87

**Table 11** The effect of NaCl and KCl salts on adsorption percentage of MIL-68(Al) for MB and MG removal

MB Removal (R%)						MG Removal (R%)					
NaCl (mol L <sup>-1</sup> )			KCl (mol L <sup>-1</sup> )			NaCl (mol L <sup>-1</sup> )			KCl (mol L <sup>-1</sup> )		
0.01	0.05	0.1	0.01	0.05	0.1	0.01	0.05	0.1	0.01	0.05	0.1
92.47	89.15	81.06	89.22	80.3	75.24	90.13	89.62	86.77	85.77	78.8	69.19

**Table 12** Comparison for the removal of MB and MG dyes by different adsorbents and methods

Adsorbent	Dye	concentration (mg L <sup>-1</sup> )	Contact time (min)	q <sup>a</sup> (mg g <sup>-1</sup> )	Refs.
Activated carbon	MB	100	30	64.30	64
Titanate nanotube	MB	50	60	94.15	65
		100	60	133.33	
Bamboo/nano zero-valent iron	MB	140	120	322.5	66
Bamboo/nano manganese	MB	140	120	263.5	66
Zeolite	MB	230	840	22.0	67
Ag-NP-AC	MB	20	10	71.4	68
Pd-NP-AC	MB	20	9.5	75.4	68
NiS-NP-AC	MB(s <sup>b</sup> )	17.8	5.46	62	69
HKUST-1 (Cu-BTC)	MB	3.2	20-360	4.88	29
c-Fe <sub>2</sub> O <sub>3</sub> /C [MIL-100(Fe)]	MB	50	30	303.95	38
MIL-100(Fe)	MG	1000	120-4320	485(T/ <sup>0</sup> C 50)	39
MIL-53(Al)-NH <sub>2</sub>	MG	5	300	164.9	70
Activated carbon (AC)	MG	15	93	4.34	71
Au-NP-AC	MG	5-85	4.4	164.57	72
ZnO-NP-AC	MG	30	15	322.58	73
Chitosan bead	MG	87.5	300	93.55	74
SWCNT		10-50	20	4.93	
SWCNT-COOH	MG	10-50	20	19.84	75
SWCNT-NH <sub>2</sub>		10-50	15	6.13	
Activated carbon synthesized from coconut coir	MG	Not reported	40	27.44	76
MWCNT-COOH	MG	50	10	11.73	77
MIL-68(Al)	MB	600	5	666.67	This study
	MG	60	5	153.85	

a- Adsorption capacity

b- simultaneous with Safranin-O

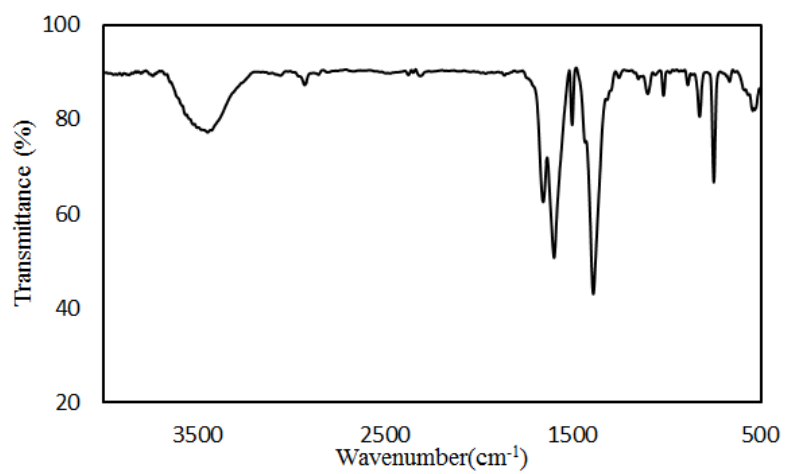


Fig.1.

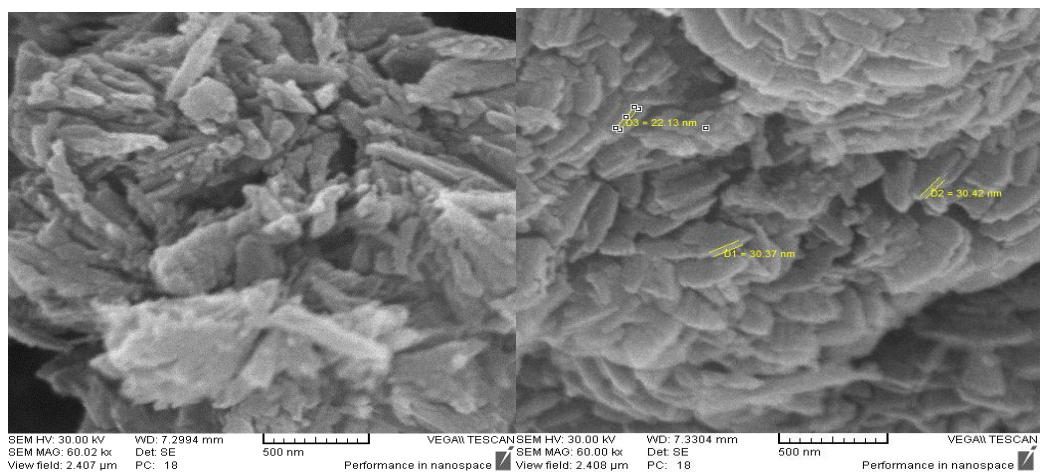


Fig.2.

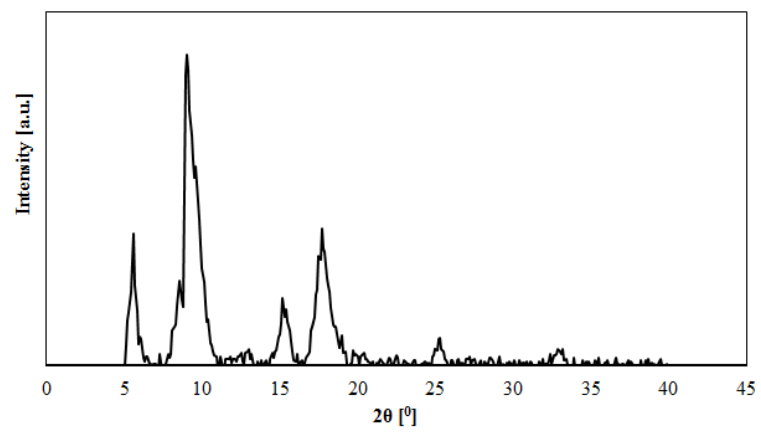


Fig.3



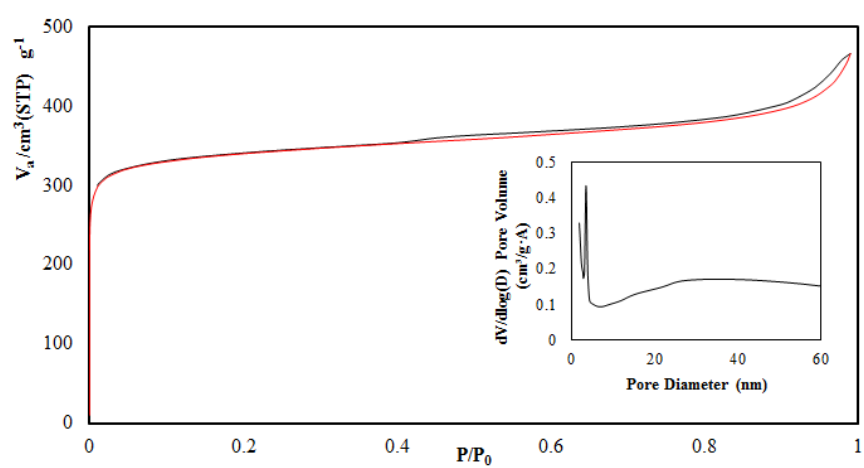


Fig.4.

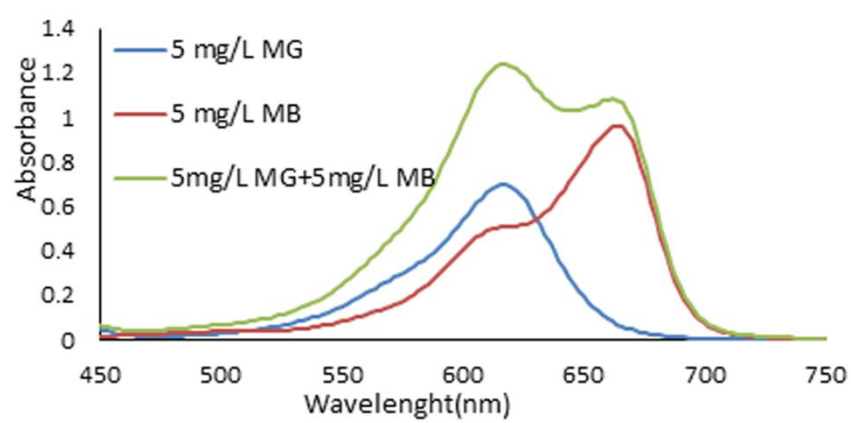


Fig.5.

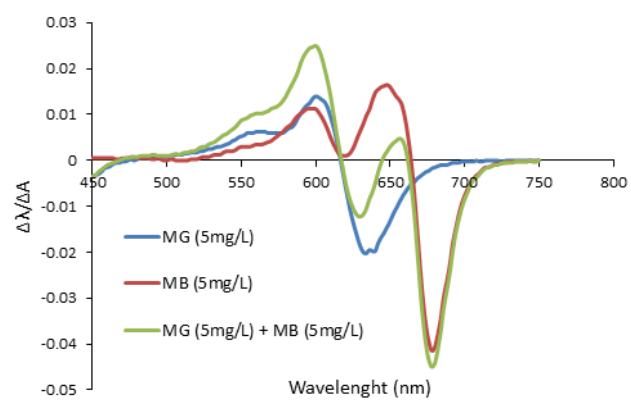


Fig.6.

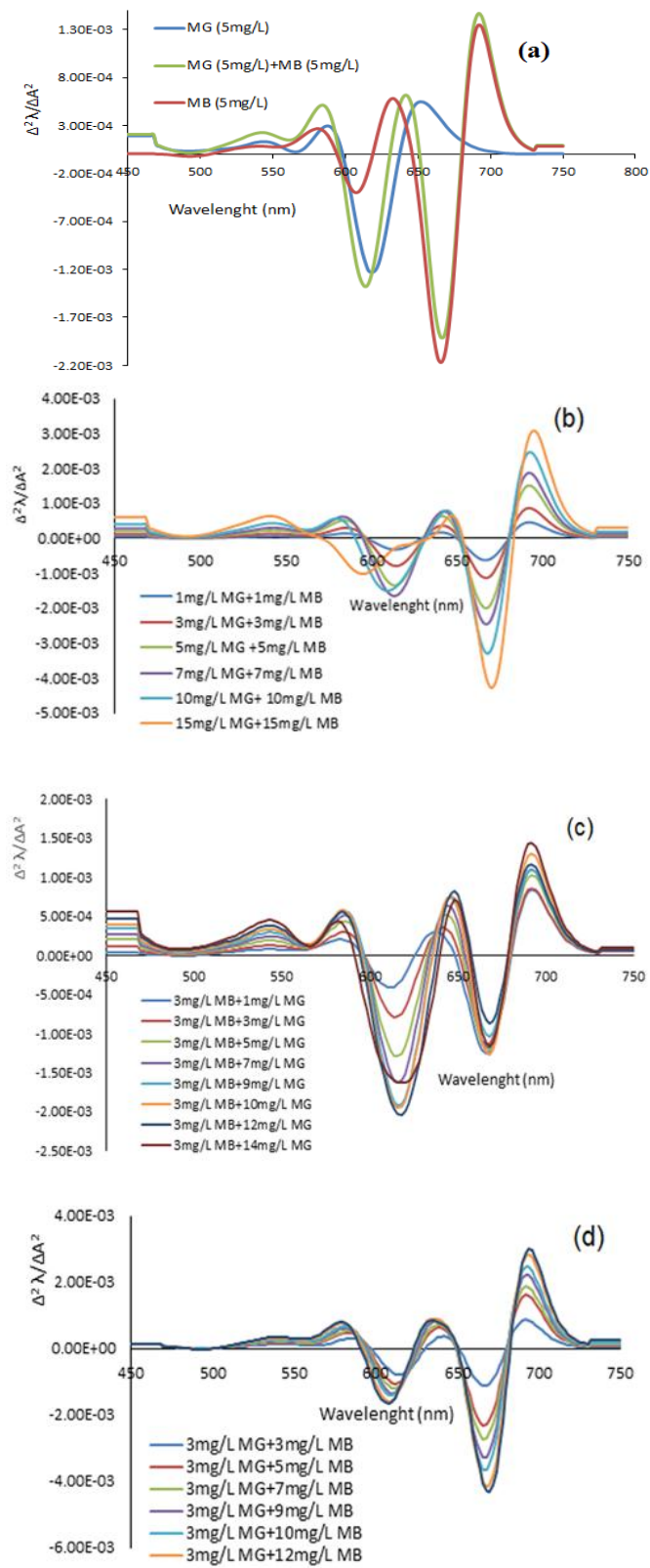


Fig. 7.

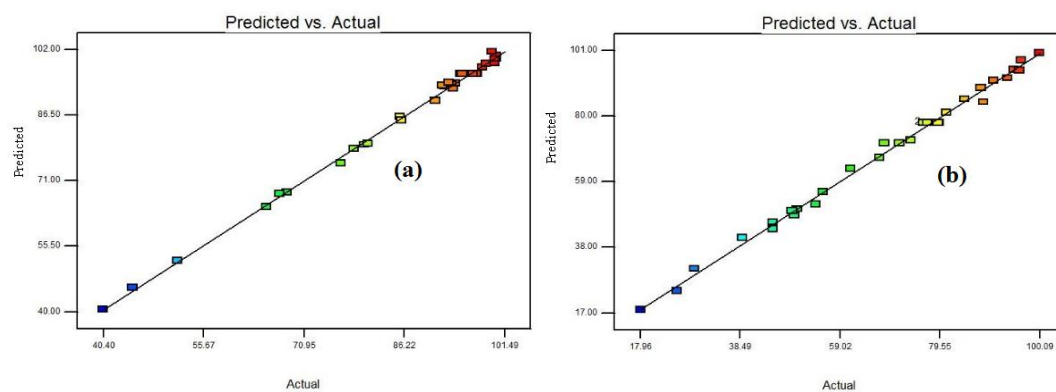


Fig. S8.

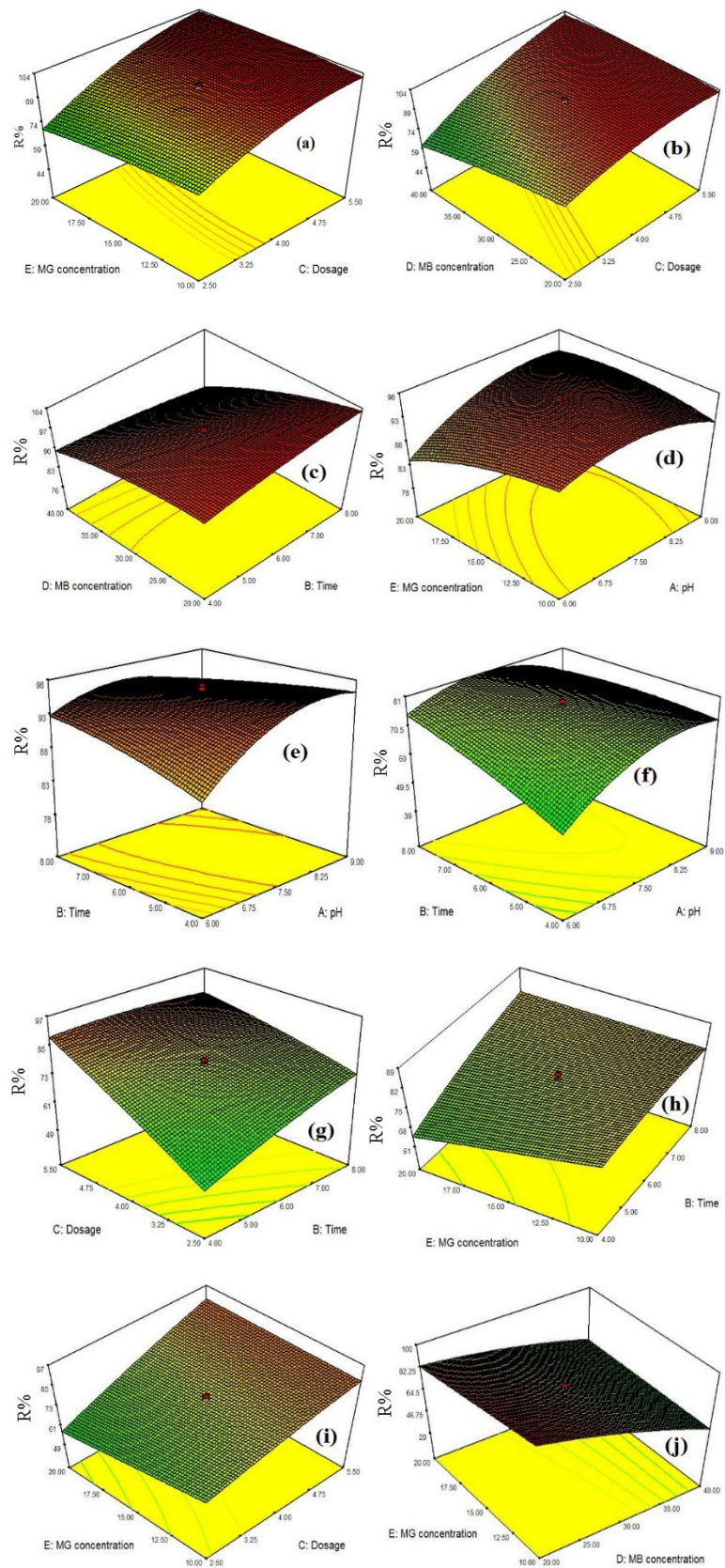


Fig.9.

